Title
Mass loss of the Amundsen Sea Embayment of West Antarctica from four independent techniques

Journal
Geophysical Research Letters, 41(23)

ISSN
0094-8276

Authors
Sutterley, Tyler C
Velicogna, Isabella
Rignot, Eric
et al.

Publication Date
2014-12-16

DOI
10.1002/2014gl061940

AGU PUBLICATIONS

Geophysical Research Letters

RESEARCH LETTER
10.1002/2014GL061940

Key Points:
- Four independent techniques of mass balance agree in the Amundsen Sea Embayment
- Most of the loss from that sector occurred in the last 10 years
- Produce regional mass balance record cross validated by four techniques

Supporting Information:
- Readme
- Figure S1
- Figure S2

Correspondence to:
T. C. Sutterley,
tsutterl@uci.edu

Citation:
Sutterley, T. C., I. Velicogna, E. Rignot, J. Mouginot, T. Flament, M. R. van den Broeke, J. M. van Wessem, and C. H. Reijmer (2014), Mass loss of the Amundsen Sea Embayment of West Antarctica from four independent techniques, *Geophys. Res. Lett.*, *41*, 8421–8428, doi:10.1002/2014GL061940.

Received 24 SEP 2014
Accepted 11 NOV 2014
Accepted article online 15 NOV 2014
Published online 15 DEC 2014

Mass loss of the Amundsen Sea Embayment of West Antarctica from four independent techniques

Tyler C. Sutterley[1], Isabella Velicogna[1,2], Eric Rignot[1,2], Jeremie Mouginot[1], Thomas Flament[3,4], Michiel R. van den Broeke[5], Jan M. van Wessem[5], and Carleen H. Reijmer[5]

[1]Department of Earth System Science, University of California, Irvine, California, USA, [2]Jet Propulsion Laboratory, California Institute of Technology, Pasadena, California, USA, [3]LEGOS, Observatoire Midi-Pyrnes, Toulouse, France, [4]Now at School of Earth and Environment, University of Leeds, Leeds, UK, [5]Institute for Marine and Atmospheric Research, Utrecht University, Utrecht, Netherlands

Abstract We compare four independent estimates of the mass balance of the Amundsen Sea Embayment of West Antarctica, an area experiencing rapid retreat and mass loss to the sea. We use ICESat and Operation IceBridge laser altimetry, Envisat radar altimetry, GRACE time-variable gravity, RACMO2.3 surface mass balance, ice velocity from imaging radars, and ice thickness from radar sounders. The four methods agree in terms of mass loss and acceleration in loss at the regional scale. Over 1992–2013, the mass loss is 83 ± 5 Gt/yr with an acceleration of 6.1 ± 0.7 Gt/yr^2. During the common period 2003–2009, the mass loss is 84 ± 10 Gt/yr with an acceleration of 16.3 ± 5.6 Gt/yr^2, nearly 3 times the acceleration over 1992–2013. Over 2003–2011, the mass loss is 102 ± 10 Gt/yr with an acceleration of 15.7 ± 4.0 Gt/yr^2. The results reconcile independent mass balance estimates in a setting dominated by change in ice dynamics with significant variability in surface mass balance.

1. Introduction

The glaciers flowing into West Antarctica's Amundsen Sea Embayment (ASE) are a focal point of glaciological studies due to their rapid acceleration, large negative mass balance, and unstable bed configuration [*Hughes*, 1973; *Rignot*, 1998, 2001]. The ASE glaciers flow with some of the highest surface velocities in the continent while draining a catchment that receives high rates of snowfall [*Rignot et al.*, 2011a; *Mouginot et al.*, 2014; *van den Broeke et al.*, 2006; *Lenaerts et al.*, 2012; *Medley et al.*, 2014]. Observations from satellite radar interferometry have shown significant surface velocity increases on the Pine Island (PIG) and Thwaites (THW) glaciers since the 1990s in conjunction with significant retreats of their grounding line positions [*Rignot*, 1998, 2001; *Rignot et al.*, 2002, 2014]. Increased mass fluxes from the smaller regional glaciers of Smith (SMI), Kohler (KOH), Pope (POP), and Haynes (HAY) have also contributed significantly to the overall acceleration in ice mass discharge into the embayment [*Thomas et al.*, 2004; *Rignot et al.*, 2008; *Mouginot et al.*, 2014]. *Mouginot et al.* [2014] report a 77% increase in total ice discharge of the ASE (145 ± 22 Gt/yr increase) between 1973 and 2013, with 50% of the discharge increase occurring between 2003 and 2009. Elevation measurements of PIG have shown strong and accelerated dynamic thinning over areas of fast flow, extending from the calving front to the upper tributaries [*Park et al.*, 2013; *Pritchard et al.*, 2009; *Flament and Rémy*, 2012]. This sector has been identified as the largest contributor from Antarctica to present-day global sea level rise using gravity data and the mass budget method [*Rignot et al.*, 2011b]. Projections from ice sheet numerical models suggest that the region will continue to be a considerable source of global sea level rise over the next century [*Seroussi et al.*, 2014; *Joughin et al.*, 2014; *Favier et al.*, 2014]. Still differences remain among published mass balance estimates for the ASE [*Shepherd et al.*, 2002; *Zwally et al.*, 2005; *Rignot et al.*, 2008; *Sasgen et al.*, 2013; *Medley et al.*, 2014]. In particular, radar altimeter estimates [*Shepherd et al.*, 2002; *Zwally et al.*, 2005] are typically lower than estimates from the mass budget method [*Rignot et al.*, 2008]. These discrepancies can be partially resolved by comparing data over the same time period and the same region but prior to this research had not yet been done.

Here we examine, during the overlapping periods, the mass balance of the ASE using four independent methods: (1) satellite time-variable gravity, (2) mass budget method (MBM), (3) satellite radar altimetry, and (4) satellite and airborne laser altimetry. We use 12 years of time-variable gravity measurements from the

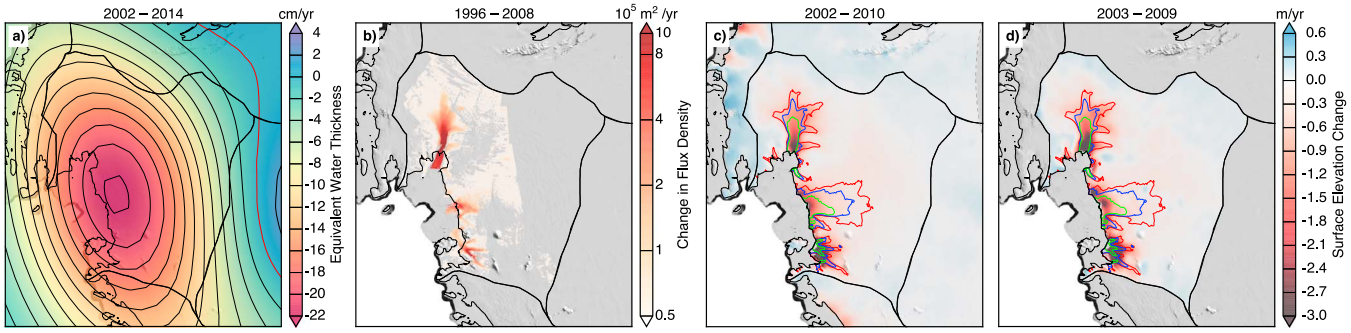

Figure 1. (a) Ice mass trend estimated using GRACE time-variable gravity in centimeter of water equivalent. The red contour delineates 0 cm yr^{-1}. (b) Change in ice flux density between 1996 and 2008 combining velocity changes from *Mouginot et al.* [2014] and ice thickness from *Rignot et al.* [2014]. (c) Elevation change estimated using repeat Envisat radar altimetry from *Flament and Rémy* [2012]. (d) Elevation change from laser altimetry combining ICESat-1 (GLAS) with Operation IceBridge (ATM and LVIS). Contours on Figures 1c and 1d denote surface ice speeds of 125 (red), 250 (blue), and 500 (green) m/yr from *Rignot et al.* [2011a]. Plots are overlaid on a MODIS mosaic of Antarctica [*Haran et al.*, 2013].

NASA/DLR GRACE (Gravity Recovery and Climate Experiment) satellite mission, 22 years of ice discharge from interferometric synthetic aperture radar (InSAR) data and surface mass balance (SMB) output products from the Regional Atmospheric Climate Model (RACMO2.3) [*van Wessem et al.*, 2014], ice thickness data derived from Operation IceBridge (OIB) radio echo sounding, 9 years of radar altimetry data from the European Space Agency Environmental Satellite (Envisat) mission, 7 years of laser altimetry data from ICESat, and 3 years from OIB. We determine the differences between the different methods in terms of mass balance, $dM(t)/dt$, and acceleration in mass balance, d^2M/dt^2, and conclude with a reconciled and comprehensive estimate of the ASE contribution to sea level in 1992–2014 evaluated using multiple techniques.

2. Data and Methods

We use 135 monthly GRACE Release-5 (RL05) gravity solutions provided by Center for Space Research (CSR) for the period April 2002 to May 2014 [*Bettadpur*, 2012]. Each CSR solution consists of fully normalized spherical harmonic coefficients ($C_{\ell m}$, $S_{\ell m}$) up to degree, ℓ, and order, m, 60. We substitute the GRACE-derived C_{20} coefficients with monthly estimates from satellite laser ranging [*Cheng et al.*, 2013], and we account for the variation of the Earth's geocenter using degree 1 coefficients provided by *Swenson et al.* [2008]. Leakage effects from outside the ice sheet are calculated as described in *Velicogna and Wahr* [2013]. We correct the GRACE mass changes for glacial isostatic adjustment (GIA), the Earth's viscoelastic response to the glacial unloading over the past several thousand years using GIA coefficients from *Ivins et al.* [2013] regional ice deglaciation model. We smooth the corrected GRACE spherical harmonics using a 250 km radius Gaussian averaging function [*Jekeli*, 1981], and we generate regular latitude-longitude monthly ice mass grids. We use the grids to calculate the linear trend in a least squares regression simultaneously fitting annual and semiannual signals [*Velicogna*, 2006; *Wahr et al.*, 1998] to obtain digital maps of ice mass balance for the ASE (Figure 1a).

We generate time series of ice mass balance for ASE by applying the least squares mass concentration (mascon) approach described in *Velicogna et al.* [2014] to the Antarctic Ice Sheet. To do this, we cover the entire ice sheet with a set of equal-area mascons (Figure S1 in the supporting information). Each mascon is a 3° diameter spherical cap with a mass equal to a uniformly distributed centimeter of water [*Farrell*, 1972; *Sutterley et al.*, 2014]. For each mascon, we calculate a set of Stokes coefficients, which we smooth with a 250 km Gaussian function and convert into mass. We simultaneously fit the mascon Stokes coefficients to the monthly GIA-corrected GRACE coefficients to obtain estimates of the monthly mass variability for each mascon. This procedure retrieves scaled estimates of regional ice mass variation at each time step. We calculate the mass anomaly time series, $M(t)$, for the ASE through summation of the regional mascons. To calculate dM/dt, we first smooth the mass anomaly time series to remove annual variations and then calculate the derivative over 13 month windows using a Savitzky-Golay filter [*Velicogna*, 2009; *Savitzky and Golay*, 1964]. Uncertainty in the GRACE estimates of ice mass changes are a combination of GRACE measurement error, leakage error, GIA uncertainty, and statistical uncertainty. Errors are calculated as described in *Velicogna et al.* [2014].

Ice mass balance from the mass budget method (MBM) is calculated combining estimates of ice discharge (D) with surface mass balance (SMB) for each drainage basin as in [*Rignot et al.*, 2011b]. For ice discharge, we use the measurements provided in *Mouginot et al.* [2014]. For SMB, we use the monthly products calculated from a 1979–2013 climate simulation of RACMO2.3 [*Ligtenberg et al.*, 2013; *van Wessem et al.*, 2014]. Field data have been used to estimate the RACMO absolute precision [*van de Berg et al.*, 2006]. In the Antarctic, the uncertainty (1σ) in SMB over grounded ice averages 7% or 144 Gt/yr [*Lenaerts et al.*, 2012]. In ASE, the uncertainty in SMB increases to 14.8% or 28 Gt/yr [*Rignot et al.*, 2008]. RACMO2.3 products are available through December 2013. To compare the results with GRACE, the rates of ice discharge are linearly interpolated into a set of monthly fluxes assuming that seasonal variations in regional ice velocity are minimal, which has been verified over short time periods. We calculate the monthly dM/dt time series by subtracting D from SMB. We generate monthly anomaly time series, $M(t)$, from the MBM by subtracting ice discharge monthly rates from surface mass balance monthly rates and calculating the cumulative $M(t)$ time series.

We use along-track repeat Envisat radar altimetry measurements from the Laboratoire d'Etudes en Géophysique et Océanographie Spatiales at the Le Centre National de la Recherche Scientifique [*Flament and Rémy*, 2012]. The along-track altimetry technique increases the number of processed data points on the Antarctic ice sheet compared to the traditional crossover analysis. We use 83 cycles of 35 day repeat orbits retrieved over the period September 2002 to October 2010. Relative surface elevations are calculated for 500 m radius disks using a least squares algorithm which simultaneously solves for radar waveform properties, along-track slope, cross-track slope, regional surface curvature assuming a quadratic shape, and the elevation time series [*Flament and Rémy*, 2012; *Rémy and Parouty*, 2009]. The waveform properties are computed using the ice sheet-optimized ICE-2 retracking algorithm, which solves for leading edge amplitude, leading edge width, trailing edge slope, waveform backscatter coefficient, and the corrected range [*Legrésy et al.*, 2005]. Additional corrections to account for the varying electromagnetic properties of the ice sheet surface are also included [*Flament and Rémy*, 2012; *Rémy and Parouty*, 2009]. Seasonal variations in radar penetration due to snowpack properties may still account for part of the seasonal signal in ice sheet elevation. To compare with GRACE, we use the Envisat individual elevation time series obtained every kilometer along track to build monthly 25 km^2 grids for the same dates used by the GRACE fields when the Envisat data are available on the 35 day repeat orbit. Error estimates for each grid point are calculated as described in [*Flament and Rémy*, 2012]. Figure 1c shows the map of surface elevation change from Envisat for the period September 2002 to October 2010. We use the two-step smoothing and Savitzky-Golay differentiation procedure previously described in the GRACE analysis to calculate the dV/dt time series.

We also use elevation measurements from ICESat-1, Operation IceBridge (OIB) Airborne Topographic Mapper (ATM) and Land, Vegetation and Ice Sensor (LVIS) to quantify the surface elevation change. Our ICESat measurements are Release-33 of the GLA12 Antarctic and Greenland Ice Sheet Altimetry data provided by the National Snow & Ice Data Center (NSIDC) [*Zwally et al.*, 2012]. We remove cloud-affected data points following the methods described in *Howat et al.* [2008], *Pritchard et al.* [2009], *Smith et al.* [2009], and *Sørensen et al.* [2011]. Elevation changes are calculated in reference to the WGS-84 ellipsoid, corrected for saturation effects with the GLA12 correction product [*Zwally et al.*, 2012], and for Gaussian-Centroid (G-C) offset [*Borsa et al.*, 2014]. OIB ATM, and LVIS data products are used as additional constraints to the surface shape and elevation time series [*Krabill*, 2010; *Blair and Hofton*, 2010]. We use a least squares approach to simultaneously solve for the elevation time series and surface shape (e.g., along-track and cross-track slope) of 1 km surface patches [*Schenk and Csatho*, 2012]. The OIB aerial laser altimetry data sets greatly increase the total number and spatial coverage of elevation data points within each surface patch [*Schenk and Csatho*, 2012; *Rezvan-Behbahani*, 2012]. For the temporal component, a low-order polynomial is chosen to reduce the impact of annual variations, which may not be captured in the two to three campaign acquisitions per year. Errors for each time step are calculated propagating the regression fit error as described in *Schenk and Csatho* [2012], and the GIA uplift uncertainty. From our reconstructed centroid time series, we calculate interpolated maps of relative surface elevation using inverse multiquadric radial basis functions and calculate elevation change maps by differentiating sets of interpolated elevation maps [*Hardy*, 1971]. Figure 1d shows the map of surface elevation change from ICESat/IceBridge for the period 2003–2009.

In order to convert the surface elevation measurements from Envisat and ICESat/OIB into ice mass, we apply a simple density conversion assuming that the surface changes in areas of fast flow (speed greater than about 50 m/yr) are entirely due to ice dynamics, i.e., are taking place at a density of 900 ± 20 kg/m^3

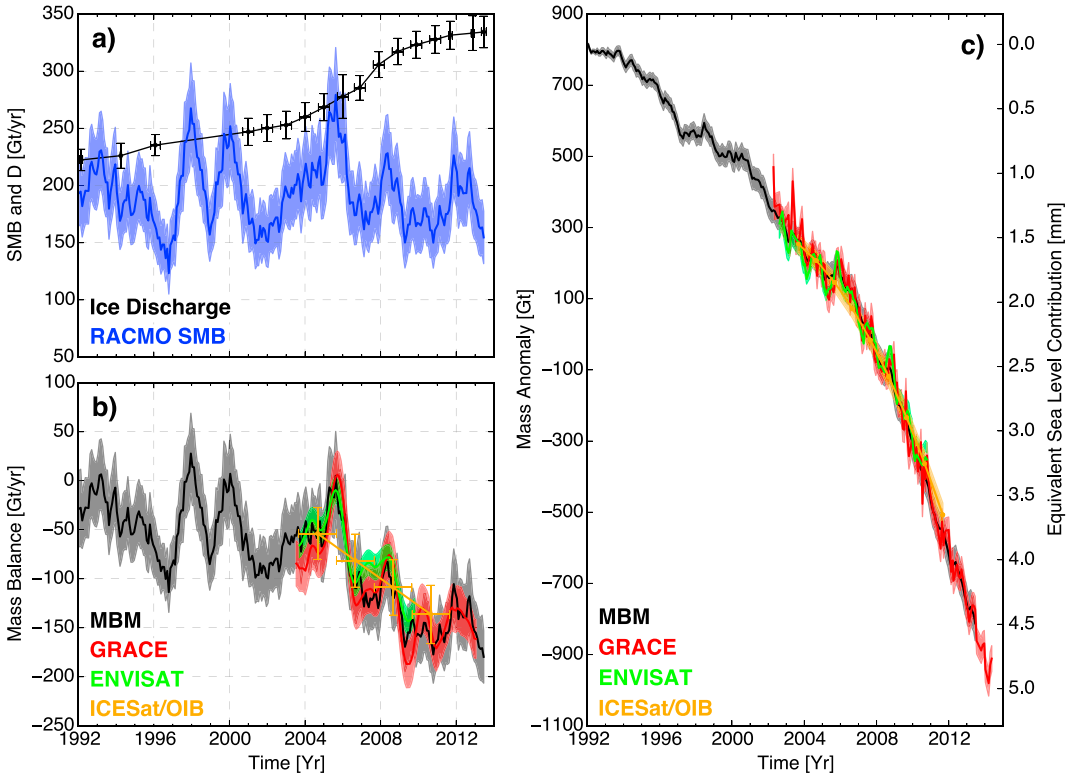

Figure 2. (a) Rates of RACMO surface mass balance, SMB (blue), and ice discharge, D, from *Mouginot et al.* [2014] (black). (b) Mass balance estimates, d$M(t)/dt$, and (c) cumulative mass anomalies, $M(t)$, for the Amundsen Sea Embayment (ASE) of Antarctica from the Mass Budget Method, MBM (black), GRACE time-variable gravity (red), Envisat radar altimetry (green), and ICESat/IceBridge laser altimetry (orange).

[*Shepherd et al.*, 2012]. This assumption is justified by the fact that changes in surface elevation (Figures 1c and 1d) are strongly correlated with the changes in speed (Figure 1b), not with changes in SMB. In slower-moving regions, changes in surface elevation are assumed to be dominated by changes in SMB rather than ice dynamics (the latter is also not observable over the entire domain). Over the slow-moving interior, we employ a density of 550 ± 250 kg/m^3, i.e., we include a 45% uncertainty. Our final error combines the errors from both regions.

3. Results

Figure 1 shows the map of GRACE ice mass trend for January 2003 to May 2014, the change in ice flux density (product of ice velocity by ice thickness) between 1996 and 2008 combining ice motion from InSAR with ice thickness from BEDMAP2 [*Fretwell et al.*, 2013], Envisat radar altimetry dH/dt for 2002–2010 and ICESat, OIB, and LVIS dH/dt for 2003–2009. GRACE trend (Figure 1a) shows a significant mass loss in the region, with a loss per unit area exceeding 20 cm water equivalent per year. The limited spatial resolution of the GRACE data (~350 km) compared to the size of the glaciers limits the interpretation of the spatial pattern of ice mass change.

The map of flux density change (Figure 1b) highlights the speed up of all glaciers in the region: PIG, THW, SMI, KOH, POP, and HAY [*Mouginot et al.*, 2014]. The maps of surface elevation change from Envisat (Figure 1c) and ICESat/OIB (Figure 1d) indicate that ASE is dominated by ice thinning. The rate of thinning is higher in regions of fast flow, as denoted by the velocity magnitude contours from *Rignot et al.* [2011a], and areas of larger change in flow speed in Figure 1b. We find thinning of PIG propagating upstream, broad thinning of THW, and significant thinning of the smaller HAY, SMI, POP, and KOH. The rates of surface thinning exceed several meters per year in the areas of fast flow, and the spatial pattern of thinning is consistent with the pattern of ice velocity change. This confirms that the pattern of thinning is due to changes in ice dynamics instead of changes in SMB.

Table 1. Mass Balance of the Amundsen Sea Embayment of West Antarctica[a]

Data Set	Date Range	Mass Balance (Gt/yr)	Change in Mass Balance (Gt/yr^2)
GRACE	2003–2009	-90 ± 8	-16.4 ± 2.6
MBM	2003–2009	-89 ± 7	-19.6 ± 3.5
Envisat	2003–2009	-74 ± 8	-15.5 ± 3.6
ICESat/OIB	2003–2009	-81 ± 16	-13.8 ± 9.6
GRACE	2003–2011	-104 ± 7	-15.5 ± 1.7
MBM	2003–2011	-105 ± 6	-18.0 ± 2.3
ICESat/OIB	2003–2011	-95 ± 14	-13.8 ± 6.3
GRACE	2003–2013	-108 ± 7	-11.9 ± 1.3
MBM	2003–2013	-110 ± 6	-13.6 ± 1.9
MBM	1992–2013	-83 ± 5	-6.1 ± 0.7

[a]Mean mass balance and change in mass balance calculated for each period simultaneously using a weighted least squares regression from the mass balance time series, $dM(t)/dt$.

Because of the inherent difference in spatial resolution and temporal coverage between the different data sets, it is difficult to compare the spatial pattern of the mass balance results. Instead, we focus on the basin-scale assessment of mass balance. During the entire time period (1992–2013), variations in SMB modulate the $dM(t)/dt$ time series significantly (Figure 2a). The average SMB for this time period is 185 ± 26 Gt/yr; yet interannual variations in SMB up to 150 Gt are not uncommon in the GRACE, Envisat, and MBM time series (Figure 2b).

During the common period, 2003–2009, GRACE, MBM, and Envisat mass balance time series, $dM(t)/dt$, are in good agreement in terms of total magnitude and timing of the cyclic oscillations (Figure 2b). The three $dM(t)/dt$ time series agree within $\pm 13\%$. Over the same period, the GRACE, Envisat, and MBM time series of cumulative mass anomaly, $M(t)$, agree within $\pm 5\%$ (Figure 2c).

The ICESat/OIB time series does not capture interannual variations because of its low temporal sampling (two to three measurements per year). Over the period common to all four techniques, 2003–2009, however, we find an excellent agreement with all the other techniques in terms of average mass balance and acceleration in mass balance. We find a total mass loss of 81 ± 16 Gt/yr for ICESat/OIB, 90 ± 8 Gt/yr for GRACE, 89 ± 7 Gt/yr for MBM, and 74 ± 8 Gt/yr for Envisat. During the same period, the acceleration in loss are, respectively, 13.8 ± 9.6 Gt/yr^2 for ICESat/OIB, 16.4 ± 2.6 Gt/yr^2 for GRACE, 19.6 ± 3.4 Gt/yr^2 for MBM, and 15.5 ± 3.6 Gt/yr^2 for Envisat (Table 1).

We calculate a reconciled mass balance for the ASE during 2003–2009 as a linear average of the individual estimates from GRACE, MBM, Envisat, and ICESat/OIB and the associated error as the sum in quadrature of each technique error. We find a rate of mass loss of 84 ± 10 Gt/yr with an average acceleration of 16.3 ± 5.6 Gt/yr^2. For comparison, over the entire period of 1992–2013, the mass loss of ASE as determined by the MBM averages 83 ± 5 Gt/yr with an acceleration of 6.1 ± 0.7 Gt/yr^2, or almost 3 times less than in the more recent period.

Over the time period 2003–2011, we have coincident data sets from ICESat/OIB, GRACE, and MBM. We find a mass loss of 95 ± 14 Gt/yr for ICESat/OIB, 104 ± 7 Gt/yr for GRACE, and 105 ± 6 Gt/yr for MBM. During the same time period, the acceleration in mass loss is 13.8 ± 6.3 Gt/yr^2 for ICESat/OIB, 15.5 ± 1.7 Gt/yr^2 for GRACE, and 18 ± 2.3 Gt/yr^2 for MBM (Table 1). This period includes the ICESat period (2003–2009) and the period of yearly OIB campaigns (2009–2011) when ICESat is no longer available. During 2003–2011, our reconciled estimate from GRACE, MBM, and ICESat/OIB is an average mass loss of 102 ± 10 Gt/yr with an acceleration of 15.7 ± 4.0 Gt/yr^2, which is not significantly different for that in 2003–2009.

4. Discussion

The excellent agreement and high correlation between independent time series from GRACE, MBM, Envisat, and ICESat/OIB during their common period significantly increases confidence in the various analyzed techniques. The coincidence in magnitude and temporal oscillations of the time series provides a significant cross validation of the techniques at the regional scale in a glaciological setting where mass changes are

significant. The agreement within the confidence intervals confirms that the error estimates for the different techniques are realistic. Beyond the end of the MBM, Envisat, and ICESat/OIB record (mid-2012), the ongoing GRACE time series of $M(t)$ measurements (Figure 2c) indicate that the mass loss of the ASE is continuing at the same rate after 2012 until the middle of year 2014 which is the end of our current GRACE record. As new SMB estimates are produced and longer time series of OIB laser data are acquired, we will extend the duration and quality of the ice sheet mass balance record in the region.

Our mass balance numbers are within the error estimates of the recent CryoSat-2 estimates from [*McMillan et al.*, 2014] who report a mass loss of 120 ± 18 Gt/yr for the time period 2010–2013 for basins 21 and 22, the equivalent of ASE in this study. For comparison, we calculate an average mass loss of 144 ± 7 Gt/yr from the linear average of GRACE and MBM in 2010–2013. The lower number from CryoSat-2 is likely due to the variability in firn depth and snowfall affecting the short-term (3 year) Cryosat-2 time series. Overall, however, the mass balance estimates agree within confidence intervals.

Although the ICESat/OIB mass balance time series do not capture interannual variations in ice elevation, our results suggest that it correctly captures the total change in mass balance of the ASE. Hence, campaign-style measurements by OIB, combined with the long-term reference from ICESat, are sufficient to extend the time series of laser altimetry data in time and maintain a consistent record of ice mass balance in the region. In our estimate, we only use the OIB data within 1 km of the ICESat tracks. The elevation change results could be improved by including additional ATM and LVIS tracks acquired in the region since 2002, but the statistical analysis would become significantly more complex. With our approach, we confirm that the resulting numbers are already consistent with those obtained with more comprehensive, complementary, independent MBM and GRACE techniques.

In the ASE, the choice of the GIA correction only minimally impacts the GRACE mass balance estimates. Here we use the *Ivins et al.* [2013] regional GIA model. Using any of the other available GIA changes the mass balance numbers by 8% or 9 Gt/yr for the *Whitehouse et al.* [2012] model and 2% or 2 Gt/yr for the *A et al.* [2013] global model based on ICE-5G ice history [*Peltier*, 2004]. These errors are within the uncertainty bounds of the reconciled estimates. Results using GIA coefficients from the *Whitehouse et al.* [2012] deglaciation model are included in the supporting information (Figure S2).

The Envisat and ICESat/OIB results fall within the error estimates of the GRACE and MBM time series when changes in surface elevation in areas of fast flow (speed greater than about 50 m/yr) are assumed to be taking place at the density of ice, here 900 ± 20 kg/m^3, i.e., to be due to ice dynamics, and changes in slower-moving regions are assumed to occur at 550 ± 250 kg/m^3, i.e., to be dominated by changes in SMB rather than ice dynamics. Overall, most change in mass in the ASE occur at low elevation (97% of the loss is contained below 1300 m elevation) and at high speed (87% of the loss for areas flowing above 50 m/yr), where changes are very likely to take place at the density of ice. We note that Envisat measurements may miss some of the coastal region due to loss of signal along the edges of the ice sheet typical of satellite radar altimeters.

The ASE receives high rates of snowfall compared to the average in Antarctica [*Lenaerts et al.*, 2012; *Medley et al.*, 2014]. In 1992–2013, the RACMO2.3 SMB averages 185 ± 26 Gt/yr for the ASE. SMB varies significantly over short time scales (σ = 27 Gt/yr in 2002–2013). Over the entire 22 year period, however, changes in SMB are negligible, −0.2 ± 0.3 Gt/yr^2 (Figure 2a). Our study confirms that multidecadal periods of observation are needed to determine the long-term trend in ice mass balance and its acceleration and to minimize the impact of firn compaction on altimetry results [*Rignot et al.*, 2011b; *Shepherd et al.*, 2012; *Wouters et al.*, 2013]. Similarly, it is difficult to evaluate the exact partitioning between SMB and ice dynamics over short periods. For example, the partitioning in mass balance over 2003–2009 does not reflect the partitioning over 1992–2013.

The longer MBM record and its comparison with independent techniques provides evidence that the increase in regional mass loss is caused almost entirely by changes in ice velocity. The long-term (1992–2013) change in SMB (−0.2 ± 0.3 Gt/yr^2) is small compared to the change in ice discharge (+5.7 ± 0.4 Gt/yr^2) (Figure 2a). The SMB fluctuations modulate the yearly mass balance yet never mask out the trend in dynamic loss in the region. Most of the ice mass loss took place in the past decade. The cumulative loss of 1160 ± 30 Gt during the 2002–2013 GRACE period is 71% of the total loss of 1630 ± 30 Gt for the 1992–2013

period. The losses correspond to equivalent rises of global sea level of 3.2 ± 0.1 mm and 4.5 ± 0.1 mm for the 2002–2013 and 1992–2013 periods, respectively (Figure 2c).

5. Conclusion

In this study, we quantify the ice sheet mass balance of the ASE using four independent geodetic techniques. We find an excellent agreement in mass loss and acceleration in mass loss from these independent techniques during common periods at the regional scale in a sector that dominates the mass balance of the continent. We show that OIB campaign style measurements are sufficient to extend the time series of mass balance estimates using ICESat laser altimetry data in time and maintain a record of ice mass balance in the region. We also show that the significant fluctuations in SMB observed over short periods average out after a couple of decades. The comprehensive record, evaluated from multiple techniques, of mass loss in West Antarctica, produced here shows a tripling in mass loss in recent years with respect to the entire analyzed period 1992–2013. The rapid rate of convergence of the independent techniques examined herein indicates that the measurements have now reached maturity and may be used with increased confidence for glaciological interpretation and inclusion in ice sheet numerical models with data assimilation methods.

Acknowledgments

This work was performed at UCI, JPL-Caltech, and LEGOS-Toulouse. It was partially supported by the NASA's Cryosphere, Terrestrial Hydrology, IDS, MEASURES Programs, contracts JPL-1390432, UTA12-000609, UTA13-000917, and the Netherlands Polar Program. Data used in this manuscript are available upon request to the authors or from NSIDC.

The Editor thanks two anonymous reviewers for their assistance in evaluating this paper.

References

A, G., J. Wahr, and S. Zhong (2013), Computations of the viscoelastic response of a 3-D compressible Earth to surface loading: An application to Glacial Isostatic Adjustment in Antarctica and Canada, *Geophys. J. Int.*, *192*(2), 557–572, doi:10.1093/gji/ggs030.

Bettadpur, S. (2012), UTCSR level-2 processing standards document, *Tech. Rep. GRACE 327-742*, Cent. for Space Res., Univ. of Texas, Austin.

Blair, J. B., and M. Hofton (2010), *IceBridge LVIS L2 Geolocated Surface Elevation Product*, NASA DAAC at NSIDC, Boulder, Colo., version 1.

Borsa, A. A., G. Moholdt, H. A. Fricker, and K. M. Brunt (2014), A range correction for ICESat and its potential impact on ice-sheet mass balance studies, *The Cryosphere*, *8*(2), 345–357, doi:10.5194/tc-8-345-2014.

Cheng, M., B. D. Tapley, and J. C. Ries (2013), Deceleration in the Earth's oblateness, *J. Geophys. Res. Solid Earth*, *118*, 740–747, doi:10.1002/jgrb.50058.

Farrell, W. E. (1972), Deformation of the Earth by surface loads, *Rev. Geophys. Space Phys.*, *10*(3), 761–797, doi:10.1029/RG010i003p00761.

Favier, L., G. Durand, S. L. Cornford, G. H. Gudmundsson, O. Gagliardini, F. Gillet-Chaulet, T. Zwinger, A. J. Payne, and A. M. Le Brocq (2014), Retreat of Pine Island Glacier controlled by marine ice-sheet instability, *Nat. Clim. Change*, *4*(2), 117–121, doi:10.1038/nclimate2094.

Flament, T., and F. Rémy (2012), Dynamic thinning of Antarctic glaciers from along-track repeat radar altimetry, *J. Glaciol.*, *58*(211), 830–840, doi:10.3189/2012JoG11J118.

Fretwell, P., et al. (2013), Bedmap2: Improved ice bed, surface and thickness datasets for Antarctica, *The Cryosphere*, *7*(1), 375–393, doi:10.5194/tc-7-375-2013.

Haran, T., J. Bohlander, T. Scambos, and M. Fahnestock (2013), *MODIS Mosaic of Antarctica 2004 (MOA2004) Image Map*, Natl. Snow and Ice Data Cent., Boulder, Colo., doi:10.7265/N5ZK5DM5.

Hardy, R. L. (1971), Multiquadric equations of topography and other irregular surfaces, *J. Geophys. Res.*, *76*(8), 1905–1915, doi:10.1029/JB076i008p01905.

Howat, I. M., B. E. Smith, I. R. Joughin, and T. A. Scambos (2008), Rates of southeast Greenland ice volume loss from combined ICESat and ASTER observations, *Geophys. Res. Lett.*, *35*, L17505, doi:10.1029/2008GL034496.

Hughes, T. (1973), Is the West Antarctic ice sheet disintegrating?, *J. Geophys. Res.*, *78*(33), 7884–7910.

Ivins, E. R., T. S. James, J. Wahr, E. J. O Schrama, F. W. Landerer, and K. M. Simon (2013), Antarctic contribution to sea level rise observed by GRACE with improved GIA correction, *J. Geophys. Res. Solid Earth*, *118*, 3126–3141, doi:10.1002/jgrb.50208.

Jekeli, C. (1981), Alternative methods to smooth the Earth's gravity field, *Tech. Rep. 327*, Ohio State Univ., Department of Geodetic Science and Surveying, 1958 Neil Avenue, Columbus, Ohio 43210, grant Number NGR37-008-161, OSURF Project 783210.

Joughin, I., B. E. Smith, and B. Medley (2014), Marine ice sheet collapse potentially under way for the Thwaites Glacier Basin, West Antarctica, *Science*, *344*(6185), 735–738, doi:10.1126/science.1249055.

Krabill, W. B. (2010), *IceBridge ATM L2 Icessn Elevation, Slope, and Roughness*, NASA DAAC at NSIDC, Boulder, Colo., version 1.

Legrésy, B., F. Papa, F. Rémy, G. Vinay, M. van den Bosch, and O.-Z. Zanife (2005), ENVISAT radar altimeter measurements over continental surfaces and ice caps using the ICE-2 retracking algorithm, *Remote Sens. Environ.*, *95*(2), 150–163, doi:10.1016/j.rse.2004.11.018.

Lenaerts, J. T. M., M. R. van den Broeke, W. J. van de Berg, E. van Meijgaard, and P. Kuipers Munneke (2012), A new, high-resolution surface mass balance map of Antarctica (1979–2010) based on regional atmospheric climate modeling, *Geophys. Res. Lett.*, *39*, L04501, doi:10.1029/2011GL050713.

Ligtenberg, S. R. M., W. J. Berg, M. R. Broeke, J. G. L. Rae, and E. Meijgaard (2013), Future surface mass balance of the Antarctic ice sheet and its influence on sea level change, simulated by a regional atmospheric climate model, *Clim. Dyn.*, *41*(3–4), 867–884, doi:10.1007/s00382-013-1749-1.

McMillan, M., A. Shepherd, A. Sundal, K. Briggs, A. Muir, A. Ridout, A. Hogg, and D. Wingham (2014), Increased ice losses from Antarctica detected by CryoSat-2, *Geophys. Res. Lett.*, *41*, 3899–3905, doi:10.1002/2014GL060111.

Medley, B., et al. (2014), Constraining the recent mass balance of Pine Island and Thwaites glaciers, West Antarctica, with airborne observations of snow accumulation, *The Cryosphere*, *8*(4), 1375–1392, doi:10.5194/tc-8-1375-2014.

Mouginot, J., E. J. Rignot, and B. Scheuchl (2014), Sustained increase in ice discharge from the Amundsen Sea Embayment, West Antarctica, from 1973 to 2013, *Geophys. Res. Lett.*, *41*, 1576–1584, doi:10.1002/2013GL059069.

Park, J. W., N. Gourmelen, A. Shepherd, S. W. Kim, D. G. Vaughan, and D. Wingham (2013), Sustained retreat of the Pine Island Glacier, *Geophys. Res. Lett.*, *40*, 2137–2142, doi:10.1002/grl.50379.

Peltier, W. R. (2004), Global glacial isostasy and the surface of the ice-age Earth: The ice-5G (VM2) model and grace, *Annu. Rev. Earth Planet. Sci.*, *32*(1), 111–149, doi:10.1146/annurev.earth.32.082503.144359.

Pritchard, H. D., R. J. Arthern, D. G. Vaughan, and L. A. Edwards (2009), Extensive dynamic thinning on the margins of the Greenland and Antarctic ice sheets, *Nature*, *461*(7266), 971–975, doi:10.1038/nature08471.

Rémy, F., and S. Parouty (2009), Antarctic ice sheet and radar altimetry: A review, *Remote Sens.*, *1*(4), 1212–1239, doi:10.3390/rs1041212.
Rezvan-Behbahani, S. (2012), Temporal history of ice dynamics contribution to volume changes of the southeast Greenland Ice Sheet, MS thesis, Dep. of Geol. Sci., Univ. at Buffalo, New York.
Rignot, E., J. Mouginot, M. Morlighem, H. Seroussi, and B. Scheuchl (2014), Widespread, rapid grounding line retreat of Pine Island, Thwaites, Smith and Kohler glaciers, West Antarctica from 1992 to 2011, *Geophys. Res. Lett.*, *41*, 3502–3509, doi:10.1002/2014GL060140.
Rignot, E. J. (1998), Fast recession of a West Antarctic glacier, *Science*, *281*(5376), 549–551, doi:10.1126/science.281.5376.549.
Rignot, E. J. (2001), Evidence for rapid retreat and mass loss of Thwaites Glacier, West Antarctica, *J. Glaciol.*, *47*(157), 213–222, doi:10.3189/172756501781832340.
Rignot, E. J., D. G. Vaughan, M. Schmeltz, T. Dupont, and D. MacAyeal (2002), Acceleration of Pine Island and Thwaites Glaciers, West Antarctica, *Ann. Glaciol.*, *34*, 189–194, doi:10.3189/172756402781817950.
Rignot, E. J., J. L. Bamber, M. R. van den Broeke, C. H. Davis, Y. Li, W. J. van de Berg, and E. van Meijgaard (2008), Recent Antarctic ice mass loss from radar interferometry and regional climate modelling, *Nat. Geosci.*, *1*(2), 106–110, doi:10.1038/ngeo102.
Rignot, E. J., J. Mouginot, and B. Scheuchl (2011a), Ice flow of the Antarctic ice sheet, *Science*, *333*(6048), 1427–1430, doi:10.1126/science.1208336.
Rignot, E. J., I. Velicogna, M. R. van den Broeke, A. J. Monaghan, and J. T. M. Lenaerts (2011b), Acceleration of the contribution of the Greenland and Antarctic ice sheets to sea level rise, *Geophys. Res. Lett.*, *38*, L05503, doi:10.1029/2011GL046583.
Sasgen, I., H. Konrad, E. R. Ivins, M. R. van den Broeke, J. L. Bamber, Z. Martinec, and V. Klemann (2013), Antarctic ice-mass balance 2003 to 2012: Regional reanalysis of GRACE satellite gravimetry measurements with improved estimate of glacial-isostatic adjustment based on GPS uplift rates, *The Cryosphere*, *7*(5), 1499–1512, doi:10.5194/tc-7-1499-2013.
Savitzky, A., and M. J. E. Golay (1964), Smoothing and differentiation of data by simplified least squares procedures, *Anal. Chem.*, *36*(8), 1627–1639, doi:10.1021/ac60214a047.
Schenk, T., and B. M. Csatho (2012), A new methodology for detecting ice sheet surface elevation changes from laser altimetry data, *IEEE Trans. Geosci. Remote Sens.*, *50*(9), 3302–3316.
Seroussi, H., M. Morlighem, E. Rignot, J. Mouginot, E. Larour, M. Schodlok, and A. Khazendar (2014), Sensitivity of the dynamics of Pine Island Glacier, West Antarctica, to climate forcing for the next 50 years, *The Cryosphere*, *8*(5), 1699–1710, doi:10.5194/tc-8-1699-2014.
Shepherd, A., D. J. Wingham, and J. A. D. Mansley (2002), Inland thinning of the Amundsen Sea sector, West Antarctica, *Geophys. Res. Lett.*, *29*(10), 2-1–2-4, doi:10.1029/2001GL014183.
Shepherd, A., et al. (2012), A reconciled estimate of ice-sheet mass balance, *Science*, *338*(6111), 1183–1189, doi:10.1126/science.1228102.
Smith, B. E., H. A. Fricker, I. R. Joughin, and S. Tulaczyk (2009), An inventory of active subglacial lakes in Antarctica detected by ICESat (2003–2008), *J. Glaciol.*, *55*(192), 573–595.
Sørensen, L. S., S. B. Simonsen, K. Nielsen, P. Lucas-Picher, G. Spada, G. Adalgeirsdottir, R. Forsberg, and C. S. Hvidberg (2011), Mass balance of the Greenland ice sheet (2003–2008) from ICESat data—The impact of interpolation, sampling and firn density, *The Cryosphere*, *5*(1), 173–186.
Sutterley, T. C., I. Velicogna, B. Csatho, M. R. van den Broeke, S. Rezvan-Behbahani, and G. Babonis (2014), Evaluating Greenland glacial isostatic adjustment corrections using GRACE, altimetry and surface mass balance data, *Environ. Res. Lett.*, *9*(1), 014004, doi:10.1088/1748-9326/9/1/014004.
Swenson, S. C., D. Chambers, and J. Wahr (2008), Estimating geocenter variations from a combination of GRACE and ocean model output, *J. Geophys. Res.*, *113*, B08410, doi:10.1029/2007JB005338.
Thomas, R. H., et al. (2004), Accelerated sea-level rise from West Antarctica, *Science*, *306*(5694), 255–258, doi:10.1126/science.1099650.
van de Berg, W. J., M. R. van den Broeke, C. H. Reijmer, and E. van Meijgaard (2006), Reassessment of the Antarctic surface mass balance using calibrated output of a regional atmospheric climate model, *J. Geophys. Res.*, *111*, D11104, doi:10.1029/2005JD006495.
van den Broeke, M. R., W. J. van de Berg, and E. van Meijgaard (2006), Snowfall in coastal West Antarctica much greater than previously assumed, *Geophys. Res. Lett.*, *33*, L02505, doi:10.1029/2005GL025239.
van Wessem, J. M., et al. (2014), Improved representation of East Antarctic surface mass balance in a regional atmospheric climate model, *J. Glaciol.*, *60*(222), 761–770, doi:10.3189/2014JoG14J051.
Velicogna, I. (2006), Measurements of time-variable gravity show mass loss in Antarctica, *Science*, *311*(5768), 1754–1756, doi:10.1126/science.1123785.
Velicogna, I. (2009), Increasing rates of ice mass loss from the Greenland and Antarctic ice sheets revealed by GRACE, *Geophys. Res. Lett.*, *36*, L19503, doi:10.1029/2009GL040222.
Velicogna, I., and J. Wahr (2013), Time-variable gravity observations of ice sheet mass balance: Precision and limitations of the GRACE satellite data, *Geophys. Res. Lett.*, *40*, 3055–3063, doi:10.1002/grl.50527.
Velicogna, I., T. C. Sutterley, and M. R. van den Broeke (2014), Regional acceleration in ice mass loss from Greenland and Antarctica using GRACE time-variable gravity data, *Geophys. Res. Lett.*, doi:10.1002/2014GL061052.
Wahr, J., M. Molenaar, and F. Bryan (1998), Time variability of the Earth's gravity field: Hydrological and oceanic effects and their possible detection using GRACE, *J. Geophys. Res.*, *103*(B12), 30,205–30,229, doi:10.1029/98JB02844.
Whitehouse, P. L., M. J. Bentley, G. A. Milne, M. A. King, and I. D. Thomas (2012), A new glacial isostatic adjustment model for Antarctica: Calibrated and tested using observations of relative sea-level change and present-day uplift rates, *Geophys. J. Int.*, *190*(3), 1464–1482, doi:10.1111/j.1365-246X.2012.05557.x.
Wouters, B., J. L. Bamber, M. R. van den Broeke, J. T. M. Lenaerts, and I. Sasgen (2013), Limits in detecting acceleration of ice sheet mass loss due to climate variability, *Nat. Geosci.*, *6*(8), 613–616, doi:10.1038/ngeo1874.
Zwally, H., R. Schutz, D. Hancock, and J. Dimarzio (2012), *GLAS/ICESat L2 Antarctic and Greenland Ice Sheet Altimetry Data (HDF5)*, NASA DAAC at the Natl. Snow and Ice Data Cent., Boulder, Colo., doi:10.5067/ICESAT/GLAS/DATA205, GLA12 Version 33.
Zwally, H. J., M. B. Giovinetto, J. Li, H. G. Cornejo, M. A. Beckley, A. C. Brenner, J. L. Saba, and D. Yi (2005), Mass changes of the Greenland and Antarctic ice sheets and shelves and contributions to sea-level rise: 1992-2002, *J. Glaciol.*, *51*(175), 509–527, doi:10.3189/172756505781829007.